Poly(L-lactic acid) with the organic nucleating agent N,N,N'-tris(1H-benzotriazole) trimesinic acid acethydrazide: Crystallization and melting behavior

Yan-Hua Cai, Ying Tang, Li-Sha Zhao

Chongqing Key Laboratory of Environmental Materials and Remediation Technologies,
Chongqing University of Arts and Sciences, Chongqing 402160, People's Republic of China
Correspondence to: Y.-H. Cai (E-mail: caiyh651@aliyun.com)

ABSTRACT: N,N,N'-Tris(1H-benzotriazole) trimesinic acid acethydrazide (BD) was synthesized from 1H-benzotriazole acetohydrazide and trischloride to serve as an organic nucleating agent for the crystallization of poly(L-lactic acid) (PLLA). First, the thermogravimetric analysis of BD exhibited a high thermal decomposition temperature; this indicated that BD maybe used as a heterogeneous nucleating agent of PLLA. Then, the effect of BD on the crystallization and melting behavior of PLLA was investigated through differential scanning calorimetry, depolarized light intensity measurements, and wide-angle X-ray diffraction. The appearance of a nonisothermal crystallization peak and increases in the glass-transition temperature and the intensity of the diffraction peak suggested that the presence of BD accelerated the overall PLLA crystallization. Upon cooling at a rate of 1°C/min, the addition of just 0.5 wt % BD to PLLA increased the onset crystallization temperature from 101.4 to 111.3°C, and the nonisothermal crystallization enthalpy increased from 0.1 to 38.6 J/g. The isothermal crystallization behavior showed that the crystallization half-time of PLLA with 0.5 wt % BD (PLLA/0.5% BD) decreased from 49.9 to 1.1 min at 105°C. However, the equilibrium melting point of PLLA/0.5% BD was lower than that of the pristine PLLA; this resulted from the increasing nucleating density of PLLA. The melting behavior of PLLA/0.5% BD further confirmed that BD improved the crystallization of PLLA, and the double-melting peaks of PLLA/0.5% BD were assigned to melting–recrystallization. © 2015 Wiley Periodicals, Inc. J. Appl. Polym. Sci. **2015**, *132*, 42402.

INTRODUCTION

Biodegradable polymers are very promising substitutes for traditional petroleum-based plastics, which result in serious environmental pollution. Thus, more and more research has focused on biodegradable polymers.[1–3] Poly(L-lactic acid) (PLLA) has exhibited the dominant position in the scientific research and technological development of biodegradable polymers because of its good biodegradability, biocompatibility, easy processing, and so on.[4,5] PLLA has been adopted in more and more fields, including packaging materials and automotive interiors.[1,6,7] Moreover, PLLA as important three-dimensional printing materials and exhibit more potential applications in complex parts directly from CAD models. Hyde et al.[8] reported that slice chambers could be manufactured with PLLA in the laboratory; these represent a powerful addition to the laboratory environment. Giordano et al. investigated the mechanical properties of three-dimensional-printing PLLA parts, and the experimental results show that the maximum value of the tensile strength of the test bars fabricated with low-molecular-weight PLLA powders was higher than that for high-molecular-weight PLLA powders.

However, PLLA has some notable drawbacks, including a low crystallization degree, poor heating resistance, and embrittlement to restrict its applications; in particular, the slow crystallization rate severely affects the thermal and mechanical performance of PLLA and PLLA composites.[10,11] Improving the overall crystallization rate of PLLA is very necessary to make PLLA competitive with commercial polymers. Many inorganic compounds, such as nano-$CaCO_3$, nano-$BaSO_4$, TiO_2, SiO_2, talc, montmorillonite, and layered metal phosphonates,[12,13] have been introduced into the PLLA matrix as crystallization nucleating agents for PLLA. For example, blends of PLLA with calcium phenyl phosphonate (PPCa), zinc phenyl phosphonate (PPZn), and barium phenyl phosphonate (PPBa) were fabricated via melt blending, and the crystallization behavior indicated that three metal phosphonates could accelerate the crystallization of

PLLA. The addition of 2 wt % PPZn to PLLA decreased the crystallization half-time ($t_{1/2}$) from 29.45 min to a minimum value of 0.57 min at 130°C. The nucleating ability of PLLA incorporated with PPZn, PPCa, and PPBa decreased in the order PPZn > PPCa > PPBa.[14] Although many studies have been done to improve the crystallization of PLLA through the addition of inorganic nucleating agents, the poor compatibility of inorganic fillers and the very limited nucleating ability of small loadings make it not the most effective alternative.[15]

In recent years, more and more organic compounds were used to serve as effective nucleating agents for PLLA. First, organic nucleating agents including ethylene bis-stearamide,[16] *myo*-inositol,[17] cyanuric acid,[18] 9, 9-cresol fluorene,[19] phthalhydrazide,[20] etc., were selected from commercial organic compounds to investigate its nucleating effect for PLLA. Then, with further knowledge of structure of organic nucleating agents for PLLA, many novel organic compounds were synthesized to attempt as the nucleating agents for PLLA. Wu and his colleagues[21] synthesized a series of novel organic bisurea compounds and investigated their nucleating effect for PLLA. The crystallization nucleating efficiency showed that the crystallization nucleating ability of bisurea compounds depended on the methylene numbers, and 1, 10-(ethane-1,2-diyl)bis(3-phenylurea) exhibited the most effective crystallization nucleating effect. 2 wt % 1, 10-(ethane-1,2-diyl)bis(3-phenylurea) made the isothermal melt crystallization rate increase by 10.5 times at 140°C. In addition, benzoyl hydrazine derivatives with different methylene chain,[22] 1,3,5-trialkyl benzenetricarboxylamides,[23] substituted aryl phosphate salts,[24] methyl-3,5-disulfobenzoate dipotassium dihydrate,[25] oxalamide derivatives,[26] etc., were synthesized to serve as nucleating agent for PLLA. The amide and benzene group are very important functional group for nucleation for PLLA through analyzing the structure characteristics of commercial and synthesized nucleating agents for PLLA.

Thus, the design and synthesis of more organic nucleating agents with amide and benzene groups would be very valuable to further confirm the crystallization nucleating mechanism and to obtain promising commercial nucleating agents. In this study, the novel *N,N,N'*-tris(1H-benzotriazole) trimesinic acid acethydrazide (BD) was synthesized to be as nucleating agent for PLLA, and the crystallization and melting behavior of PLLA in the presence of BD were investigated through differential scanning calorimetry (DSC), depolarized light intensity measurements, wide-angle X-ray diffraction, and so on.

EXPERIMENTAL

Materials
PLLA was purchased from Nature Works LLC. 1H-Benzotriazole, butyl alcohol, ethanol, and hydrazine hydrate were purchased from Chengdu Kelong Chemical Reagent Co. (China). Sodium hydroxide, hydrochloric acid, and sulfuric acid were purchased from Chongqing Chuandong Chemical (Group) Co., Ltd. (China). Chloroacetic acid was purchase from Tianjin Damao Chemical Reagent Co. (China). Trimesinic acid was purchased from Energy Chemical Reagent Co. (China). *N,N*-Dimethylacetamide, thionyl dichloride, and pyridine were procured from Mianyang Rongshen Chemical Reagents Co. (China).
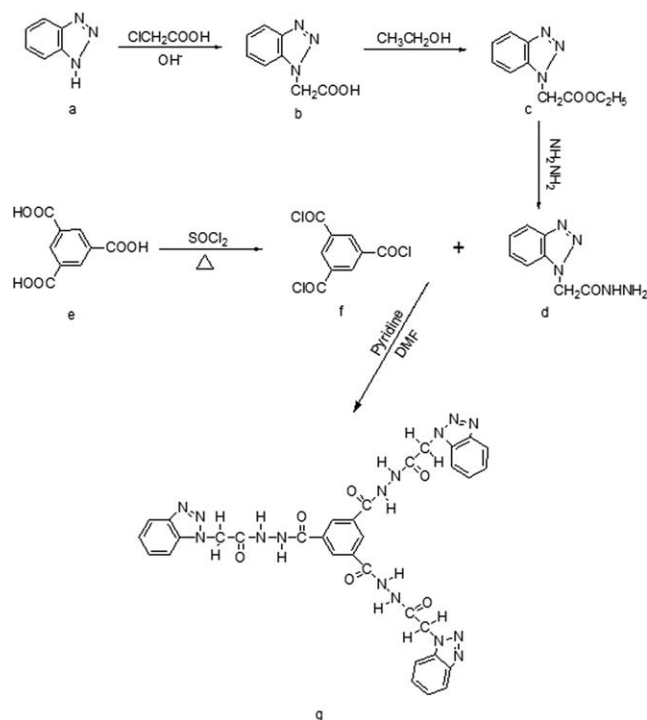
Scheme 1. Synthesis of BD.

Synthesis of BD
BD was synthesized, as shown in Scheme 1. Amounts of 0.04 mol of 1H-benzotriazole, 0.04 mol of chloroacetic acid, and 0.08 mol of sodium hydroxide in the presence of 100 mL of water were mixed, and the mixture was heated up to reflux for 3 h with stirring. The reaction mixture was filtered, and hydrochloric acid was added slowly into the filtrate; this was followed by filtrating. The obtained crude product was washed with water three times and recrystallized with butyl alcohol. The white powder of the product 1H-benzotriazole-1-ylacetic acid (product **b**) was obtained. Volumes of 8.6 mL of ethanol and 2 mL of sulfuric acid mixture were added slowly to 0.05 mol of product **b,** and the mixture was heated slowly up to reflux for 3 h with stirring. The reaction mixture was cooled to room temperature and poured into crushed ice to obtain a white deposit, and the white deposit was washed with water until it was neutral. Product **c** (1H-benzotriazole ethyl acetate) was dried at 45°C.

IR (KBr, υ, cm^{-1}): 2932.7, 1742.4, 1618.4, 1495.6, 1454.9, 1212.8, 1026.4, 744.6.

An amount of 0.015 mol of product **c,** 2 mL of 50 vol % hydrazine hydrate, and 8 mL of ethanol were mixed, the mixture was heated up to reflux for 3 h, and the white needlelike 1H-benzotriazole acetohydrazide (product **d**) was obtained after cooling to room temperature.

IR (KBr, υ, cm^{-1}): 2935.8, 1658.1, 1607.1, 1546.2, 1496.6, 1457.3, 1416, 1316.6, 1228.1, 774.9, 752.3. ^{1}H-NMR (dimethyl sulfoxide, 400 MHz, δ, ppm): 9.64 (s, 1H, NH), 7.38–8.06 (m, 4H, Ar), 5.40 (s, 2H, CH$_2$), 4.40 (s, 2H, NH$_2$).

An amount of 0.04 mol of trimesinic acid and 90 mL of thionyl dichloride in the presence of *N,N*-dimethylacetamide as a
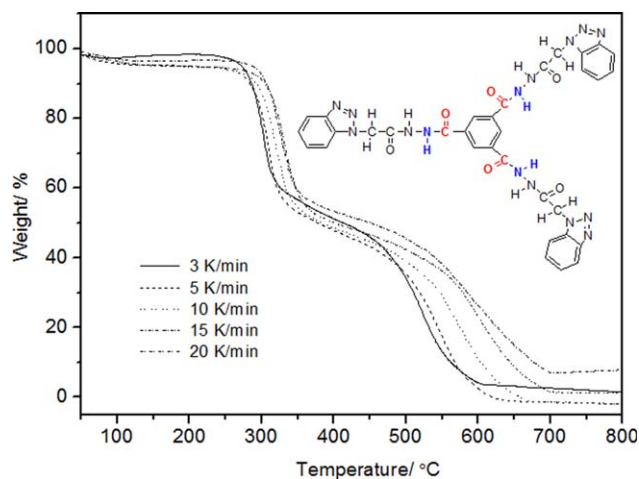
Figure 1. TGA curves of BD at different heating rates. [Color figure can be viewed in the online issue, which is available at wileyonlinelibrary. com.]

catalyst was mixed, and the mixture was heated up to 80°C and held at 80°C for 36 h with stirring. After the mixture was cooled to room temperature and thionyl dichloride was evaporated in vacuo, the residue was trischloride (product **f**).

Product **d** and 60 mL of N,N-dimethylacetamide were mixed, and trischloride was added slowly to the mixture. This was followed by the addition of pyridine, and the mixture was stirred at room temperature for 2 h and heated up to 70°C for 3 h with stirring. The reaction mixture was poured into 250 mL of water and cooled to room temperature. This was followed by filtration. The crude product was washed with water and methanol four times. The resulting product **g** (BD) was dried *in vacuo* at 45°C.

IR (KBr, υ, cm^{-1}): 3437.4, 3237.6, 1701.1, 1674.2, 1619.8, 1549.1, 1493.1, 1456.1, 1409.2, 1313.2, 1229.2, 750.2. ^{1}H-NMR (dimethyl sulfoxide, 400 MHz, δ, ppm): 10.80 (s, 6H, NH), 7.41–8.63 (m, 15H, Ar), 5.64 (s, 6H, CH$_2$).

Preparation of the PLLA/BD Sample
The blending of the dried PLLA and 0.5 wt % BD was performed in a counterrotating mixer, and the detailed blending procedure was similar to that used in our previous study.[15]

Characterization
IR Spectra. The IR spectra of BD were recorded on a Bio-Rad FTS135 spectrophotometer from 4000 to 400 cm^{-1}.

^{1}H-NMR. ^{1}H-NMR of BD was performed on a Bruker Avance 300 spectrometer. The deuterated solvent was dimethyl sulfoxide.

Thermogravimetric Analysis (TGA). TGA of BD was performed with a Thermal Analysis Q500 under air flow (60 mL/min) from room temperature to 800°C.

DSC. The nonisothermal crystallization and melting behavior of PLLA and PLLA with 0.5 wt % BD (PLLA/0.5% BD) was measured by a DSC Q2000 instrument. The nonisothermal crystallization measurement was as follows. The sample was heated to 190°C and maintained at that temperature for 3 min to ensure

that the polymer crystals were melted completely. Then, the sample was cooled from melt to 40°C at different cooling rates.

Depolarized Light Intensity Measurement. The isothermal crystallization behavior of PLLA and PLLA/0.5% BD was investigated by a GJY-III optical depolarizer in the region from 100 to 115°C.

Wide-Angle X-ray Diffraction. The wide-angle X-ray diffraction experiments of PLLA and PLLA/0.5% BD were performed on a D/MAX2550 diffractometer with Cu Kα radiation (wavelength = 1.54 Å) at room temperature in the range 2θ = 5–60 ° at a scanning rate of 2°/min.

RESULTS AND DISCUSSION

Thermal Stability of BD
The thermal stability is a very important evaluation factor for applications. Figure 1 shows the TGA curves of BD at different heating rates. As shown in Figure 1, it was clear that BD exhibited three thermal decomposition stages, and the onset decomposition temperature of BD increased with increasing heating rate; this resulted from the heat hysteresis of the high heating rate. A similar phenomenon was reported in other literature.[27] The minimum onset decomposition temperature of BD at a heating rate of 3°C/min was 285.2°C; this result is very important for BD as a nucleating agent for PLLA because the melting blend temperatures of the PLLA and PLLA composites were about 180–190°C, and the thermal decomposition temperature of BD was higher than that of the processing temperature of the PLLA and PLLA composites. This indicated that BD did not decompose in the melting blend stage of PLLA and BD.

Crystallization Behavior of PLLA/BD
The nucleating ability of BD was evaluated through a study on the effects of BD on the crystallization behavior of PLLA. Figure 2 shows the DSC curves of nonisothermal crystallization from the melt. As shown in Figure 2, the crystallization peak of the neat PLLA at a cooling rate of 1°C/min was almost not observed; this resulted from its very poor crystallization ability, and the weak crystallization peak of the neat PLLA appeared only at a lower cooling rate (see Figure 3). This also confirmed
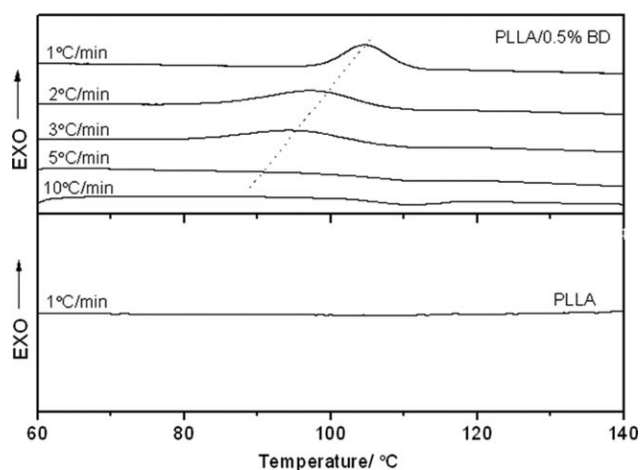

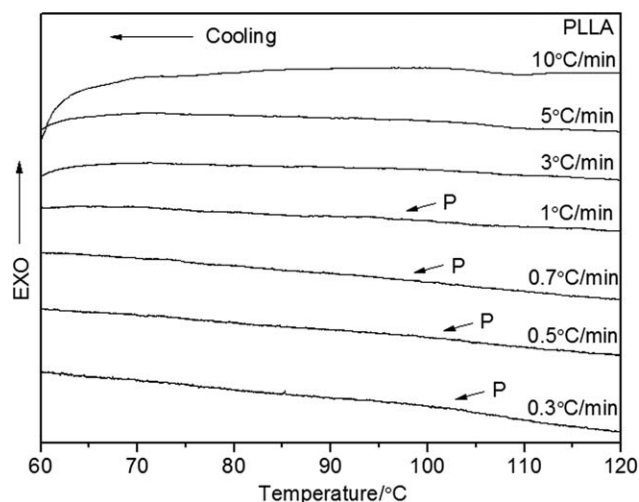**Figure 2.** DSC curves of the nonisothermal crystallization of PLLA and PLLA/0.5% BD from the melt.

Figure 3. DSC curves of the nonisothermal crystallization of PLLA at different cooling rates from the melt. P is non-isothermal crystallization peak.

Figure 4. Glass-transition temperatures of PLLA and PLLA/0.5% BD after nonisothermal crystallization.

the poor crystallization ability of the neat PLLA. However, the addition of 0.5 wt % BD gave PLLA a particularly obvious crystallization peak at a cooling rate of 1°C/min. Furthermore, the crystallization peak of PLLA/0.5% BD was also observed at a higher cooling rate; this indicated increases in the overall crystallization rate and crystalline degree during nonisothermal crystallization. This result also indicated that BD acted as a heterogeneous nucleating agent for PLLA.

It is also shown in Figure 2 that the crystallization peak for PLLA containing 0.5 wt % BD shifted to a lower temperature and became much wider with increasing cooling rate. The reason was that the increasing cooling rate resulted in more imperfect crystals during the nonisothermal crystallization procedure and the formation of large and small crystals. This result also shows that the cooling rate significantly affected the crystallization behavior of PLLA, and there existed a competition relevance between the crystallization rate and cooling rate during nonisothermal crystallization. The DSC data of PLLA and PLLA/0.5% BD crystallized from the melt are listed in Table I. Upon cooling at 1°C/min, compared to the neat PLLA, 0.5 wt % BD made the onset crystallization temperature (T_o) increase from 101.4 to 111.3°C. The crystallization peak temperature (T_{cp}) increased from 94.5 to105.2°C, and the nonisothermal crystallization enthalpy (ΔH_c) increased from 0.1 to 38.6 J/g.

In addition, the increases in the glass-transition temperature and intensity diffraction peak of PLLA/0.5% BD after nonisothermal crystallization further confirmed that BD accelerated the crystallization of PLLA (see Figures 4 and 5). The 0.5 wt % BD made the glass-transition temperature of PLLA increase from 56.5 to 60.2°C. The decrease of amorphous behavior in the PLLA/0.5% BD sample after nonisothermal crystallization made the macromolecule segment exhibit a more regular structure and more difficult active ability; this resulted in an increase in the glass-transition temperature. Figure 5 shows the X-ray diffraction curves of PLLA and PLLA/0.5% BD sample after nonisothermal crystallization at a cooling rate of 2°C/min from the melt. The PLLA exhibited a flat and wide diffraction peak, and PLLA/0.5% BD showed a very strong peak at $2\theta = 16.5°$ due to diffraction from the (110) plane and another peak at $2\theta = 18.9°$, which occurred from the (203) plane.[28] The X-ray diffraction result was consistent with the aforementioned nonisothermal crystallization results.

Table I. DSC Data for PLLA/0.5% BD Crystallized from the Melt at Different Cooling Rates

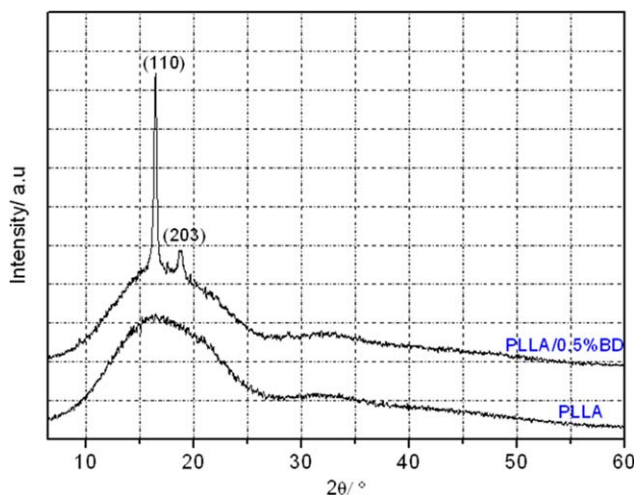| Sample	Rate (°C/min)	T_o (°C)	T_{cp} (°C)	ΔH_c (J/g)
PLLA	1	101.4	94.5	0.1
PLLA/0.5% BD	1	111.3	105.2	38.6
	2	107.8	97.3	24.3
	3	106.8	94.6	8.2
	5	106.0	96.9	0.6
	10	100.8	94.4	0.03

Figure 5. X-ray diffraction of PLLA and PLLA/0.5% BD after nonisothermal crystallization at a cooling rate of 2°C/min. [Color figure can be viewed in the online issue, which is available at wileyonlinelibrary.com.]
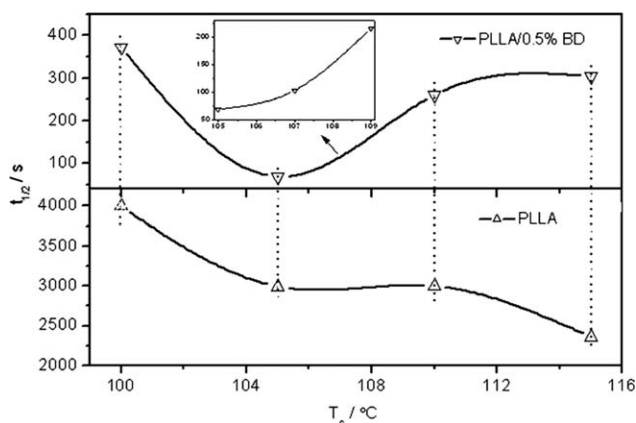
Figure 6. Curves of T_c versus $t_{1/2}$ for PLLA and PLLA/0.5% BD.

Figure 8. Melting behavior of PLLA at different heating rates corresponding to the rate of nonisothermal crystallization at different cooling rates. P is melting peak.

The isothermal crystallization behavior of PLLA and PLLA/0.5% BD was performed by depolarized light intensity measurement. Figure 6 shows the curves of the crystallization temperature (T_c) against $t_{1/2}$ for PLLA and PLLA/0.5% BD. For the neat PLLA, $t_{1/2}$ became shorter with increasing T_c in the region from 100 to 115°C, but $t_{1/2}$ was still very long. This result also confirmed that the crystallization ability of the neat PLLA was very poor. However, the addition of BD led $t_{1/2}$ to decrease first then increase and to possess a minimum value of 105°C. Compared to the neat PLLA, $t_{1/2}$ of PLLA/0.5% BD decreased from 49.9 to 1.1 min at 105°C. The direct reason was that BD improved the nucleating density of the PLLA matrix. On the other hand, this result also shows that T_c depended on $t_{1/2}$ of PLLA/0.5% BD because T_c affected the macromolecular segment active ability. Thus, $t_{1/2}$ of PLLA/0.5% BD exhibited a minimum value at 105°C.

In addition, the equilibrium melting point of PLLA and PLLA/0.5% BD could be determined with Hoffmann–Week plots.[29] Figure 7 shows a plot of the melting temperature (T_m) versus T_c of PLLA and PLLA/0.5% BD after isothermal crystallization for four $t_{1/2}$ values at different T_c's. The equilibrium melting points of PLLA and PLLA/0.5% BD were 165.35 and 163.30°C, respec-
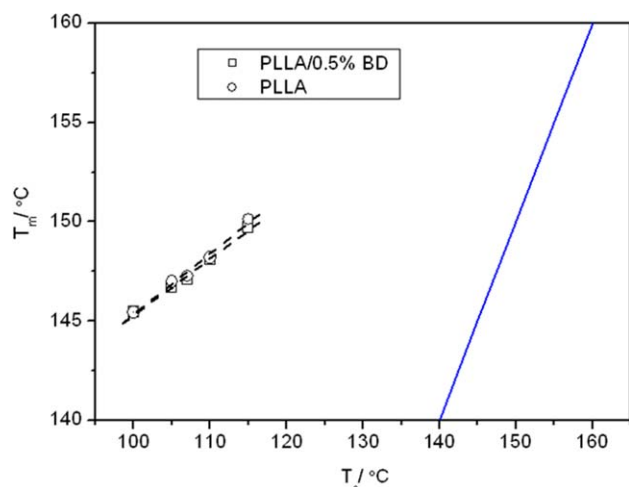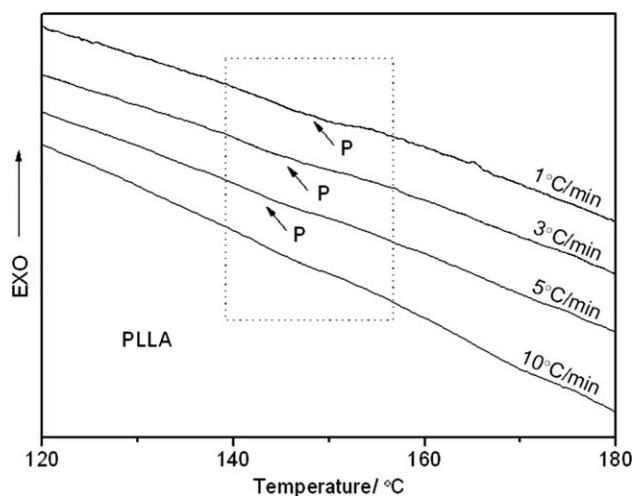
tively. It was clear that the equilibrium melting point of PLLA was higher than that of PLLA/0.5% BD; this indicated that the increasing nucleating density resulting from the presence of BD made the PLLA crystal small and more imperfect and gave rise to an ease of melting.

Melting Behavior of PLLA/BD

Additives can affect the melting behavior of a polymer matrix, and compared to the neat polymer, polymer composites exhibit different melting behaviors. Figures 8 and 9 present the melting behavior of PLLA and PLLA/0.5% BD at different heating rates that corresponded to the rates of nonisothermal crystallization at different cooling rates. It was observed, as shown in Figure 8, that PLLA had a weak melting peak at heating rates of 1, 3, and 5°C/min, but the melting peak was not observed at a heating rate of 10°C/min. The reason was that the faster rate made the PLLA macromolecule segment not form a regular structure in
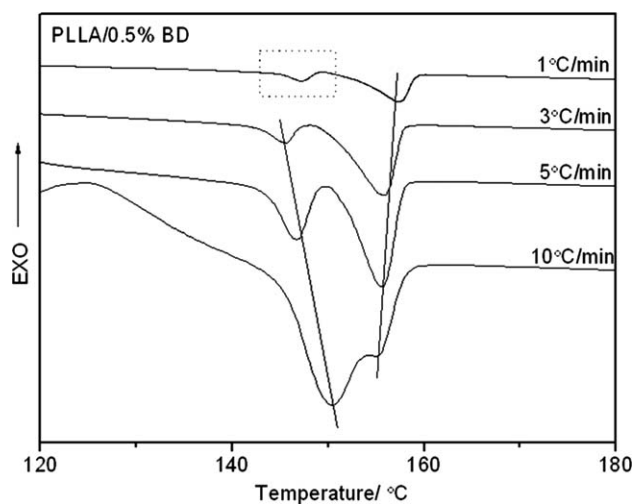

Figure 7. Plot of T_m versus T_c of PLLA and PLLA/0.5% BD. [Color figure can be viewed in the online issue, which is available at wileyonlinelibrary.com.]

Figure 9. Melting behavior of PLLA/0.5% BD at different heating rates corresponding to the rate of nonisothermal crystallization at different cooling rates.
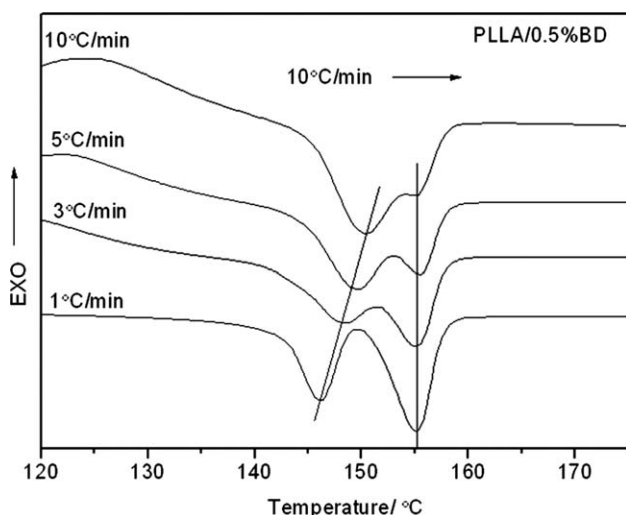
Figure 10. Melting behavior of PLLA/0.5% BD at a heating rate 10°C/min after nonisothermal crystallization at different cooling rates.

Figure 11. Melting behavior of PLLA at a heating rate of 10°C/min after sufficient crystallization. P is melting peak.

the T_c region. Thus, there existed no crystals in the PLLA matrix after nonisothermal crystallization and a second heating process; this resulted in no melting peak at high rates.

However, PLLA/0.5% BD exhibited an obvious melting peak, and there existed double-melting peaks. The double-melting peak behavior of PLLA has been reported in the literature, and two important mechanisms, including melting–recrystallization and the melting of crystals of different stability, were used to explain the double-melting peak behavior.[30] As shown in Figure 9, the low-temperature melting peak shifted to a higher temperature with increasing rate apart from 1°C/min. The possible reason was that a faster heating rate exhibited a greater thermal inertia compared with the nucleating effect of BD. However, more crystals form at a cooling rate of 1°C/min, and the formed crystals were more perfect. Thus, the melting peak of the primary formed crystals at nonisothermal crystallization at a cooling rate of 1°C/min appeared in a higher temperature region. This result shows the competition relevance of the crystallization rate and cooling rate. In addition, it is clear from Figure 9 that the shift to lower temperature occurred for the high-temperature melting peak of PLLA/0.5% BD with increasing heating rate; this was due to the decrease of the crystal number, and perfect crystals formed in the second heating process. These results indicate the double-melting peaks of PLLA/0.5% BD were assigned to melting–recrystallization. The increase in the peak area ratio of the low-temperature melting peak and high-temperature melting peak with increasing heating rate also further confirmed the decrease in the crystal number formed in the second heating process.

Figure 10 shows the melting behavior of PLLA/0.5% BD at a heating rate of 10°C/min after nonisothermal crystallization at different cooling rates. Double-melting peaks still existed, and the increase in the cooling rate of nonisothermal crystallization led to a shift in the low-temperature melting peak to a higher temperature, but the high-temperature melting peak almost did not move because the high-temperature melting peak resulted from the crystals formed in the second heating process. The
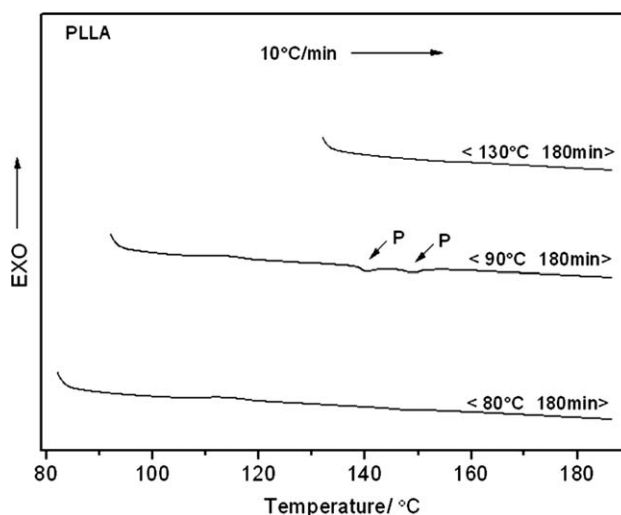
same heating rate and BD made PLLA exhibited a similar crystal number and perfect crystals.

Figures 11 and 12 show the melting behaviors of PLLA and PLLA/0.5% BD, respectively, at a heating rate of 10°C/min after sufficient crystallization in the low-temperature and high-temperature regions. Usually, PLLA exhibits a faster nuclear rate than crystal growth rate in the low-temperature region; in contrast, the crystal growth rate is faster than the nuclear rate in the high-temperature region. As shown in Figure 11, the melting peak of neat PLLA was almost not observed at a set T_c apart from 90°C; this indicated the poor nuclear ability of the neat PLLA. Compared to the neat PLLA, PLLA/0.5% BD exhibited double-melting peaks in the low-temperature region of 80–90°C (see Figure 12), and the increase in T_c made the low-temperature melting peak shift to a higher temperature. Also, ΔH_c increased from 0.5 to 4.3 J/g. These results show that the nucleating agent BD enhanced the crystallization performance
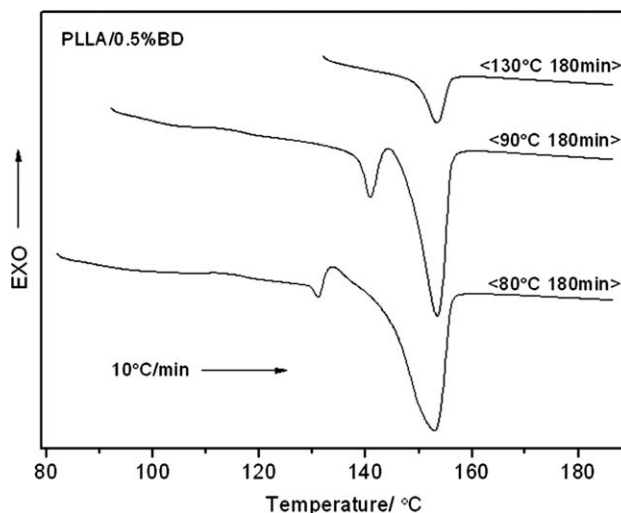

Figure 12. Melting behavior of PLLA/0.5% BD at a heating rate of 10°C/min after sufficient crystallization.

again. On the other hand, the crystallization ability of PLLA/ 0.5% BD depended on the macromolecular segment active ability in the low-temperature region. However, the PLLA/0.5% BD only exhibited one melting peak in the high-temperature region, which resulted from the few perfect crystals formed in this region.

CONCLUSIONS

BD was synthesized to be as a kind of heterogeneous nucleating agent for PLLA. The crystallization and melting behavior of PLLA/BD indicated that BD could significantly improve the crystallization performance of PLLA, the nonisothermal crystallization showed that the addition of 0.5 wt % BD made T_o increase from 101.4 to 111.3°C at a cooling rate of 1°C/min, T_{cp} increased from 94.5 to105.2°C, and ΔH_c increased from 0.1 to 38.6 J/g. The isothermal crystallization showed that $t_{1/2}$ of PLLA/0.5% BD decreased from 49.9 to 1.1 min at 105°C. The decrease in the equilibrium melting point of PLLA/0.5% BD indicated the increase in the nucleating density. The melting behavior indirectly confirmed the nucleating effect of BD, and the double-melting peaks of PLLA/0.5% BD were assigned to melting–recrystallization.

ACKNOWLEDGMENTS

REFERENCES

1. Martino, L.; Berthet, M. A.; Angellier-Coussy, H.; Gontard, N. *J. Appl. Polym. Sci.* **2015**, *132*, 41611.

2. Nakayama, Y.; Aihara, K.; Yamanishi, H.; Fukuoka, H.; Tanaka, R.; Cai, Z. G.; Shiono, T. *J. Polym. Sci. Part A: Polym. Chem.* **2015**, *53*, 489.

3. Haque, M. U. I.; Stocchi, A.; Alvarez, V.; Pracella, M. *Fibers Polym.* **2014**, *15*, 2625.

4. Li, C.; Dou, Q. *Thermochim. Acta* **2014**, *594*, 31.

5. Yan, S.; Yin, J.; Yang, Y.; Dai, Z.; Ma, J.; Chen, X. *Polymer* **2007**, *48*, 1688.

6. Vainionpaa, S. S.; Rokkanen, P.; Tormala, P. *Prog. Polym. Sci.* **1989**, *14*, 679.

7. Gu, J. D.; Gada, M.; Kharas, G.; Eberiel, D.; MaCarthy, S. P.; Gross, R. A. *Polym. Mater. Sci. Eng.* **1992**, *67*, 351.

8. Hyde, J.; MacNicol, M.; Odle, A.; Garcia-Rill, E. *J. Neurosci. Methods* **2014**, *238*, 82.

9. Giordano, R. A.; Wu, B. M.; Borland, S. W.; Cima, L. G.; Sachs, E. M.; Cima, M. J. *J. Biomater. Sci. Polym. Ed.* **1996**, *8*, 63.

10. Xiao, H. Q.; Guo, D.; Bao, J. J. *J. Appl. Polym. Sci.* **2015**, *132*, 41454.

11. Shi, J.; Lu, X. P.; Li, H. Y.; Li, D. Z. *J. Therm. Anal. Calorim.* **2014**, *117*, 1385.

12. Liao, R.; Yang, B.; Yu, W.; Zhou, C. *J. Appl. Polym. Sci.* **2007**, *104*, 310.

13. Pan, P.; Liang, Z.; Cao, A.; Inoue, Y. *ACS Appl. Mater. Interfaces* **2009**, *2*, 402.

14. Wang, S.; Han, C.; Bian, J.; Han, L.; Wang, X.; Dong, L. *Polym. Int.* **2011**, *60*, 284.

15. Cai, Y.; Yan, S.; Yin, J.; Fan, Y.; Chen, X. *J. Appl. Polym. Sci.* **2011**, *121*, 1408.

16. Harris, A. M.; Lee, E. C. *J. Appl. Polym. Sci.* **2008**, *107*, 2246.

17. Tachibana, Y.; Maeda, T.; Ito, O.; Maeda, Y.; Kunioka, M. *Polym. Degrad. Stab.* **2010**, *95*, 1321.

18. Weng, M. T.; Qiu, Z. B. *Thermochim. Acta* **2014**, *577*, 41.

19. Jin, F. Z.; Kawasaki, S. Presented at 238th ACS National Meeting [C], Washington, DC, Aug. **2009**.

20. Wang, Y.; He, D.; Wang, X.; Cao, W.; Li, Q.; Shen, C. *Polym. Bull.* **2013**, *70*, 2911.

21. Xu, Y.; Wu, L. *Eur. Polym. J.* **2013**, *49*, 865.

22. Kawamoto, N.; Sakai, A.; Horikoshi, T.; Urushihara, T.; Tobita, E. *J. Appl. Polym. Sci.* **2007**, *103*, 198.

23. Wang, T.; Yang, Y.; Zhang, C.; Tang, Z.; Na, H.; Zhu, J. *J. Appl. Polym. Sci.* **2013**, *130*, 198.

24. Shi, Y.; Shao, L.; Yang, J.; Huang, T.; Wang, Y.; Zhang, N.; Wang, Y. *Polym. Adv. Technol.* **2013**, *24*, 42.

25. Zhiqiang, S.; Han, Z.; Xuan, P.; Xinchao, B.; Wenqi, C.; Xuesi, C. *Chem. Res. Chin. Univ.* **2014**, *30*, 333.

26. Ma, P.; Xu, Y.; Wang, D.; Dong, W.; Chen, M. *Ind. Eng. Chem. Res.* **2014**, *53*, 12888.

27. Li, S.; Cai, Y. *Asian J. Chem.* **2011**, *23*, 2619.

28. De Santis, P.; Kovacs, A. J. *Biopolymers* **1968**, *6*, 299.

29. Cai, Y. *South Afr. J. Chem.* **2011**, *64*, 115.

30. Yasuniwa, M.; Satou, T. *J. Polym. Sci. Part B: Polym. Phys.* **2002**, *40*, 2411.